

Control of *Face-to-face* and Extended Aggregations of Crown Ether-Appended Metalloporphyrins

Hideyuki Shinmori,^{*,[a]} Yuzo Yasuda,^[a] and Atsuhiko Osuka^{*,[a]}

Keywords: Crown compounds / Dimerization / Fluorescence spectroscopy / NMR spectroscopy / Porphyrins

Metalloporphyrins bearing two crown ether moieties (benzo-15-crown-5) at the 5- and 15-positions have been prepared by condensation of 4'-formyl-benzo-15-crown-5 with either unsubstituted or *meso*-aryl-substituted dipyrromethanes, followed by oxidation and metallation. The *meso-meso*-coupled Zn^{II} diporphyrin **Zn4** was prepared by the oxidative coupling of **Zn1** with AgPF₆. UV/vis, fluorescence, and ¹H NMR spectroscopic studies revealed that addition of K⁺ and Rb⁺ to solutions of monomeric porphyrin derivatives **M1** (M = 2 H, Zn, Co, Ni, Pd, Cu) in CHCl₃:MeCN (2:1 v/v) induced *face-to-face* dimerization with high stability constants (ca. 10¹⁵–10¹⁹ M^{−3}). ¹H NMR analysis showed that the two **Zn1** molecules in the *face-to-face* dimer were packed more closely than in TPP-type Zn^{II} porphyrin bearing four crown ethers (Krishnan et al, *J. Am. Chem. Soc.* **1982**, *104*, 3643), but such dimeriz-

ation was hardly detected for 10,20-diphenylated Zn^{II} porphyrin **Zn2**, probably due to steric hindrance exerted by the *meso* phenyl groups. *meso*-Monoarylated Zn^{II} porphyrin **Zn3** exhibited a comparably large stability constant for formation of the *face-to-face* dimer with the *meso*-aryl substituents pointing outward. Coordination of 4-dimethylaminopyridine to Co^{II} porphyrin was shown to be stronger than the interaction of K⁺ with the crown ether, thereby dissociating the *face-to-face* dimer (**Co1**)₂ into six-coordinated monomeric Co^{II} porphyrin **5**. The diporphyrin **Zn4** formed extended linear aggregates upon addition of K⁺ and Rb⁺, owing to the divergent disposition of the crown ether substituents.

(© Wiley-VCH Verlag GmbH, 69451 Weinheim, Germany, 2002)

Introduction

Molecular assembly by means of intermolecular interactions have been of wide interest as a means for constructing large molecular architectures quickly and efficiently,^[1,2] but control of these assembling process is not necessarily easy. Among many molecules involved in assemblies, porphyrin is an attractive component because of its fascinating photophysical,^[3,4] electrochemical, catalytic,^[5] and geometrical properties.^[6–10] Porphyrin assemblies are also interesting in terms of their possible relevance to important biological proteins such as the photosynthetic reaction center, light-harvesting complexes,^[11] and cytochromes.^[12]

Here we report that K⁺-induced dimerization of benzo-15-crown-5-appended metalloporphyrins can be controlled by the introduction of peripheral substituents and the choice of central metals in the porphyrin core, and by the addition of a ligand capable of coordinating to the central metal. We also report that a skeletal change from porphyrin monomer to *meso-meso*-linked diporphyrin results in a dramatic change in the manner of assembly, from *face-to-face* dimerization to an extended aggregation into a linear supramolecular network by virtue of the divergent disposition

of the crown ethers. Krishnan et al. have reported^[9] the K⁺-induced *face-to-face* dimerization of Zn^{II} 5,10,15,20-tetrakis(benzo-15-crown-5)porphyrin (**ZnTCP**), with a stability constant of ca. 10²³ M^{−5}. It has been suggested that cooperative interaction between the crown ethers and K⁺ gives rise to such a large stability constant. The stability constant therefore decreases with a decrease in the number of the crown ethers: 10¹⁶ M^{−4} for Zn^{II} 5,10,15-tris(benzo-15-crown-5)-20-phenylporphyrin, and below noticeable levels for Zn^{II} 5,15-bis(benzo-15-crown-5)-10,20-diphenylporphyrin and Zn^{II} 5-(benzo-15-crown-5)-10,15,20-triphenylporphyrin.

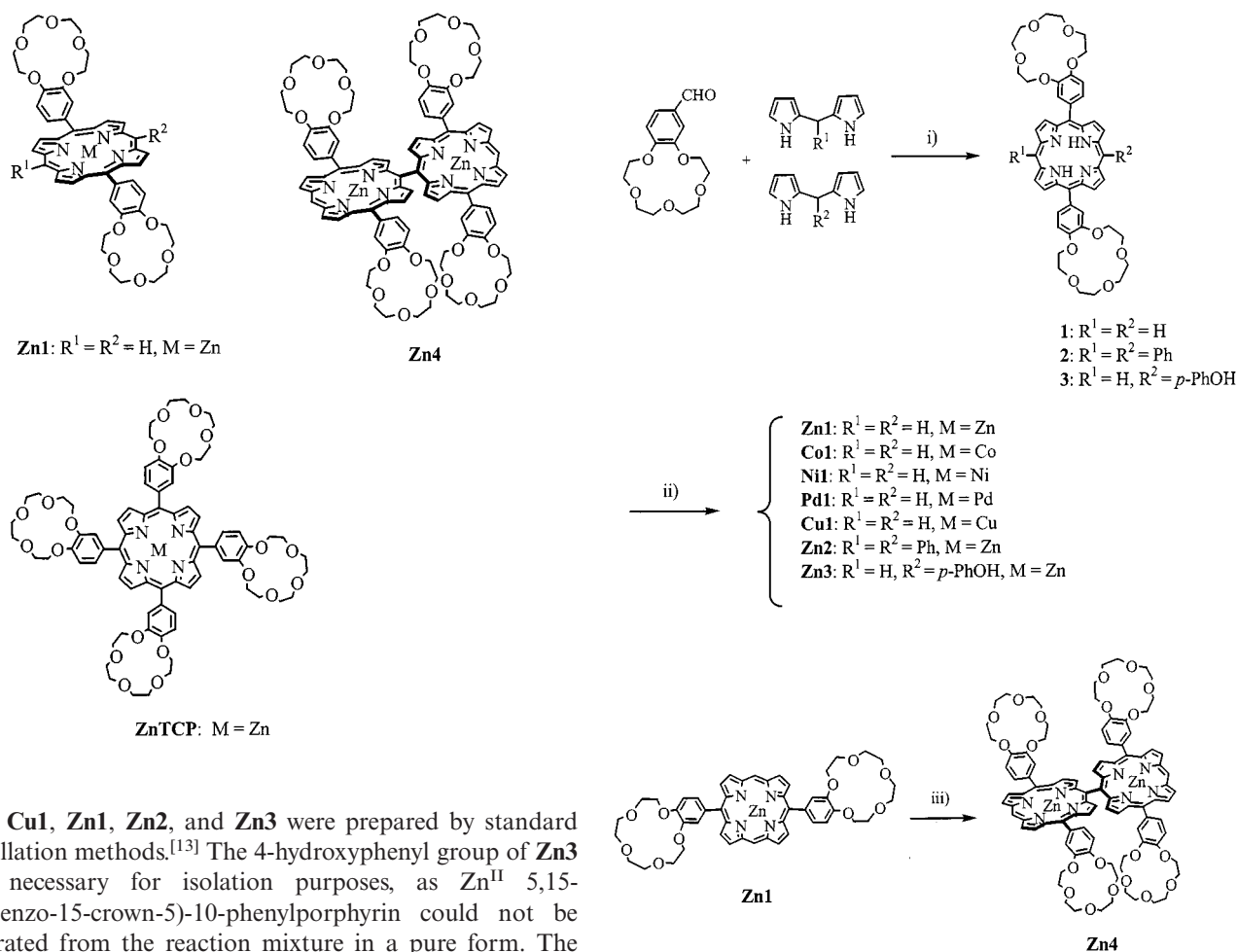
In this paper we focus on the dimerization and aggregation behavior of Zn^{II}-5,15-bis(benzo-15-crown-5)porphyrin **Zn1** and *meso-meso*-linked Zn^{II} diporphyrin **Zn4**, which lack *meso*-phenyl substituents. As described below, **Zn1** shows the larger stability constant for formation of *face-to-face* dimer, despite there being only two crown ethers available for aggregation.

Results and Discussion

Synthesis of Crown Ether-Appended Porphyrins 1–3 and *meso-meso*-Coupled Diporphyrin **Zn4**

Synthetic routes to the crown ether-appended porphyrins **1**, **2**, and **3** and the *meso-meso*-linked Zn^{II} diporphyrin **Zn4** are shown in Scheme 1. Metal complexes such as **Co1**, **Ni1**,

^[a] Department of Chemistry, Graduate School of Science, Kyoto University, Kyoto 606-8502, Japan
Fax: (internat.) + 81-75/753 3970
E-mail: shinmori@kuchem.kyoto-u.ac.jp



Scheme 1. Synthesis of crown ether-appended porphyrin and diporphyrin: i) $BF_3 \cdot Et_2O$, $CHCl_3$ then DDQ; ii) $M(OAc)_2$, $CHCl_3/MeOH$; iii) $AgPF_6/MeCN$, $CHCl_3/MeOH$

Face-to-face Dimerization of Crown Ether-Appended Porphyrins

While addition of Na^+ ions to a solution of **Zn1** in $CHCl_3/MeCN$ (2:1 v/v) did not induce any significant UV/vis or fluorescence spectral changes, addition of K^+ ions caused a noticeable blue shift of the Soret band from 415 to 396 nm, with an isosbestic point at 404 nm (Figure 1),^[14] as well as a monotonous decrease in the fluorescence intensity (Figure 2). The fluorescence quantum yields of **Zn1** and **Zn1** plus K^+ ions (7.6×10^{-5} M) determined relative to ZnTPP (0.03)^[15] are 0.022 and 0.004, respectively. These spectral changes can be explained in terms of the formation of *face-to-face* dimer (**Zn1**)₂, which was also identified by 1H NMR spectroscopy (Figure 3). The 1H NMR spectrum of (**Zn1**)₂ showed sharp signals that could be assigned to two kinds of *meso*-H signals (at $\delta = 10.27$ and 6.73) and four kinds of β -H signals (at $\delta = 9.43$, 8.89, 8.26, and 7.38) in the aromatic region, indicating that (**Zn1**)₂ had adopted a slipped *face-to-face* structure as shown in Scheme 2. The observed different chemical shifts [inner protons (*i*) and outer protons (*o*)] for the two *meso*-H and upfield-shifted β -H protons were consistent with this slipped geometry. In addition, the aromatic proton H_a in the phenyl bridge was

shifted downfield and the H_b and H_c were shifted upfield, probably suggesting fixation of the crown ether-appended phenyl bridge as shown in Scheme 2, with the H_a proton located outward and the H_b and H_c protons located inward with respect to the complexed porphyrin counterpart. This means that (**Zn1**)₂ was fixed in a *syn* conformation with both crown loops on one side of the porphyrin plane, because each aromatic proton signal (H_a , H_b , and H_c) was of one kind in the 1H NMR spectrum. The stoichiometry of the **Zn1**- K^+ ion complex was confirmed by a Job plot^[16] of the absorbance at 396 nm against $[Zn1]/([Zn1]+[K^+])$ (Figure 4), which gave a maximum at 0.50 mol/mol, indicating 1:1 or 2:2 stoichiometry. The above 1H NMR results supported the view that the stoichiometry of the **Zn1**- K^+ ion complex was 2:2. The changes in the intensity of the Soret band at 415 nm and in the fluorescence intensity of **Zn1** at 640 nm upon addition of alkali metal ions (Na^+ , K^+ , Rb^+ , and Cs^+) are depicted in Figure 5. Only marginal effects were seen for the addition of Na^+ and Cs^+ ions, while intense changes were observed for Rb^+ ions. However, the strongest influence was noted for K^+ ions. A slightly enhanced fluorescence intensity upon addition of

Figure 1 is a line graph showing the fluorescence spectra of the 1:1 complex of compound 1 and K⁺. The y-axis is labeled 'Fluorescence Intensity' and ranges from 0.0 to 2.0. The x-axis is labeled 'Wavelength /nm' and ranges from 500 to 800. The graph displays a series of overlapping fluorescence spectra for different concentrations of K⁺. The highest curve, representing 0 M K⁺, has a primary peak at approximately 640 nm with an intensity of about 1.75. A secondary peak is visible at approximately 590 nm with an intensity of about 1.1. As the concentration of K⁺ increases, the fluorescence intensity decreases across the entire spectrum. The lowest curve, representing 7.6 × 10⁻⁵ M K⁺, has a primary peak at approximately 640 nm with an intensity of about 0.85 and a secondary peak at approximately 590 nm with an intensity of about 0.4. An arrow points downwards from the 0 M curve towards the 7.6 × 10⁻⁵ M curve, indicating the direction of increasing K⁺ concentration.

$$2 \text{ Zn1} + 2 \text{ M}^+ \rightarrow (\text{Zn1})_2[\text{M}^+]_2 \quad (1)$$

Figure 1 displays two ^1H NMR spectra of poly(2-vinylpyridine) in CDCl_3 . The top spectrum, recorded before the addition of K^+ , shows peaks for *meso*-H, $\beta\text{-H}_a$, $\beta\text{-H}_b$, H_a , H_b , and H_c . The bottom spectrum, recorded after the addition of K^+ , shows peaks for outer *meso*-H, $\beta\text{-H}_{ao}$, $\beta\text{-H}_{bo}$, H_a , $\beta\text{-H}_{bi}$, $\beta\text{-H}_{ai}$, H_c , H_b , and inner *meso*-H. The x-axis represents the chemical shift δ in ppm, ranging from 11.0 to 6.5.

[illegible]

stability constants *per binding site consisting of two crown ethers and one K^+ ion*, for which the value of $\approx 10^6 \text{ M}^{-1}$ can be derived for **ZnTCP**, and that for **Zn1**, which we determined to be $\approx 10^9 \text{ M}^{-1}$, the latter is 10^3 times larger. One possible explanation for this enhancement may be that there is less steric hindrance in the *face-to-face* dimerization for **Zn1** than for **ZnTCP**. It has been demonstrated well that π - π interactions are strongest at a rather close approach (ca. 3.4–3.6 Å) of the interacting π -planes, and these are very

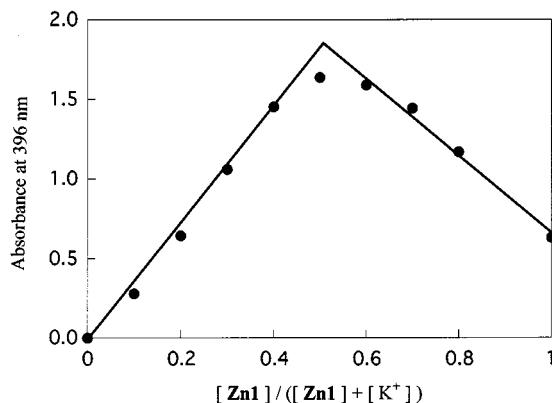


Figure 4. Job plot; $[\text{Zn1}] + [\text{K}^+] = 1.1 \times 10^{-4} \text{ M}$

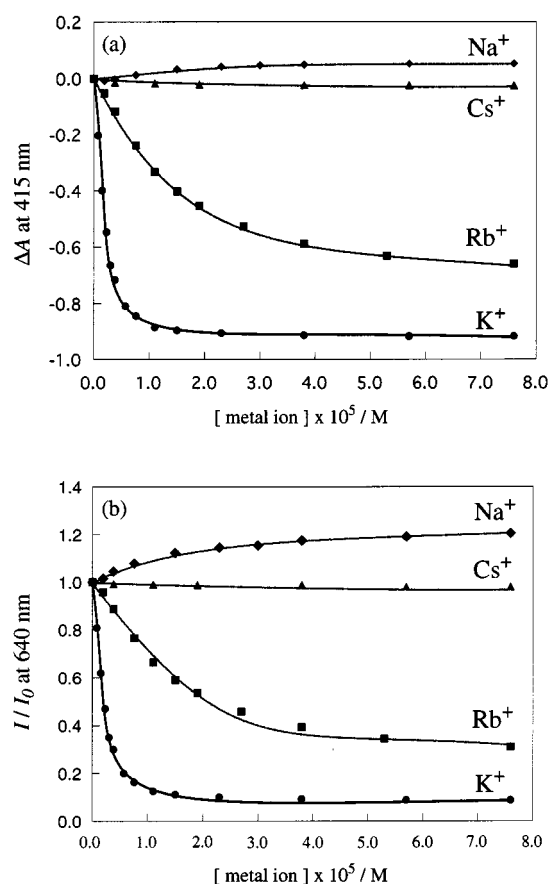


Figure 5. Plots of $[\text{metal ion}]$ against ΔA at 415 nm (a) and I/I_0 at 640 nm (b) for **Zn1** in $\text{CHCl}_3/\text{MeCN}$, 2:1 at room temperature; $[\text{Zn1}] = 1.9 \times 10^{-6} \text{ M}$, $\lambda_{\text{ex}} = 404 \text{ nm}$

sensitive to geometric changes.^[18] In view of this, bis(5,15-benzo-15-crown-5)porphyrin systems such as **Zn1** may be favorable for π - π interactions, owing to their lack of two *meso*-phenyl substituents, which exert some steric hindrance. In line with this, the observed upfield chemical shift changes, $\Delta\delta$, of the peripheral β -protons in **Zn1** were larger (2.01 ppm for $\beta\text{-H}_{\text{ai}}$ and 0.86 ppm for $\beta\text{-H}_{\text{bi}}$) than those of **ZnTCP** ($\Delta\delta$; 0.41 and 0.25 ppm for $\beta\text{-H}$). These results suggested that the interporphyrin distance was shorter in

(**Zn1**)₂ than in the dimer of **ZnTCP**, and that additional cooperative π - π interaction was giving rise to the enhancement of the stability constant of (**Zn1**)₂ per binding site.

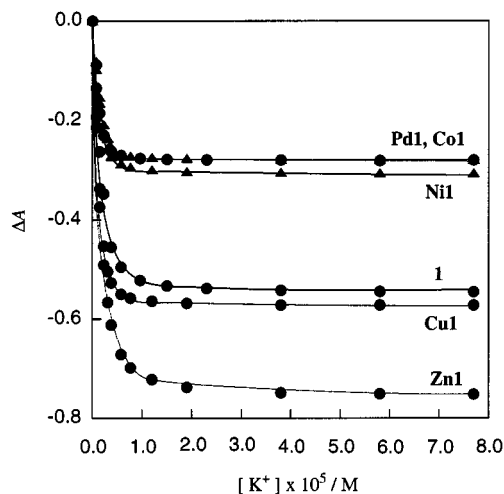


Figure 6. Plots of $[\text{K}^+]$ against ΔA for crown ether-appended metalloporphyrins in $\text{CHCl}_3/\text{MeCN}$, 2:1 at room temperature; $[\text{Metalloporphyrins}] = 1.9 \times 10^{-6} \text{ M}$

Table 1. Stability constants of crown ether-appended metalloporphyrins with potassium ion

Metalloporphyrins	$K \times 10^{18} \text{ M}^{-3}$
1	1.9 ± 0.1
Zn1	2.2 ± 0.3
Co1	3.3 ± 0.9
Ni1	3.5 ± 0.5
Pd1	1.7 ± 0.9
Cu1	18.0 ± 4.8

We next examined the dimerization behavior of **Zn2** and **Zn3**. Addition of K^+ ions to a solution of **Zn2** in $\text{CHCl}_3/\text{MeCN}$ (2:1) induced no significant change in the UV/vis and fluorescence spectra (Figure 8), consistently with Krishnan's results.^[9] The fluorescence quantum yields of **Zn2** and **Zn2** plus K^+ ions ($2.0 \times 10^{-4} \text{ M}$) determined relative to ZnTPP (0.03)^[15] were 0.020 and 0.020, respectively. This result also highlighted the sensitivity of this dimerization towards steric factors, showing that the introduction of the 10,20-diphenyl substituents posed some steric congestion that suppressed the *face-to-face* dimerization. In contrast, addition of K^+ ions to a solution of **Zn3** in $\text{CHCl}_3/\text{MeCN}$ (2:1) caused a blue shift of the Soret band from 422 to 403 nm, with an isosbestic point at 411 nm (Figure 7), as well as a decrease in the fluorescence intensity, indicating the assembly of a *face-to-face* diporphyrin (**Zn3**)₂ similar to that observed for **Zn1**. The fluorescence quantum yields of **Zn3** and **Zn3** plus K^+ ions ($9.0 \times 10^{-5} \text{ M}$) determined relative to ZnTPP (0.03)^[15] were 0.029 and 0.013, respectively. Analysis of a plot of K^+ concentration against ΔA for **Zn3** (Figure 8) revealed the stability constant to be $1.3 \pm 0.3 \times 10^{17} \text{ M}^{-3}$, similar to the values for the 5,15-bis(benzo-15-crown-5)porphyrin systems. This

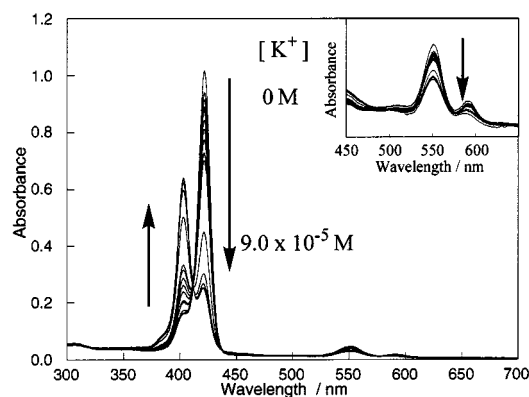


Figure 7. Absorption spectra **Zn3** on addition of KClO_4 in $\text{CHCl}_3/\text{MeCN}$, 2:1 at room temperature; $[\text{Zn3}] = 1.9 \times 10^{-6} \text{ M}$

dimerization process was also studied by ^1H NMR (Table 2), which revealed a large upfield shift of the *meso*-H signal from $\delta = 10.13$ to $\delta = 6.84$, combined with a splitting of the β -H signals: two β -H signals were observed at high-field chemical shifts ($\delta = 8.22$ and 7.44) while another set of β -H signals were shifted only slightly upfield, appearing at $\delta = 9.02$ and $\delta = 8.74$. These results were consistent with the formation of a slipped, offset *face-to-face* dimer (**Zn3**)₂, in which the *meso*-aryl substituents were directed outward to avoid steric hindrance. It may therefore be concluded that K^+ ions can trigger the dimerization

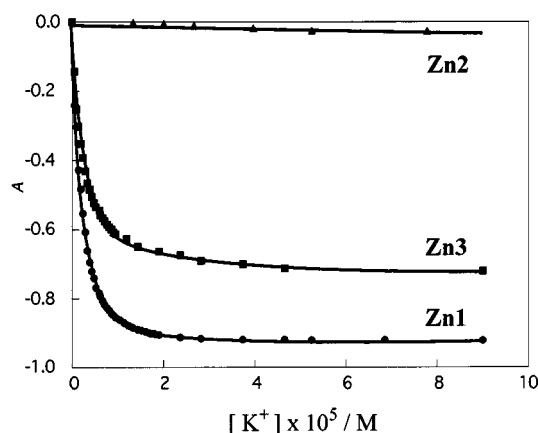


Figure 8. Plots of $[\text{K}^+]$ against ΔA for **Zn1** at 415 nm; **Zn2** at 425 nm, and **Zn3** at 422 nm in $\text{CHCl}_3/\text{MeCN}$, 2:1 at room temperature; $[\text{Zn1}] = [\text{Zn2}] = [\text{Zn3}] = 1.9 \times 10^{-6} \text{ M}$

of 5,15-bis(benzo-15-crown-5) Zn^{II} -porphyrin in a restricted offset geometry without a substantial reduction in the stability constant.

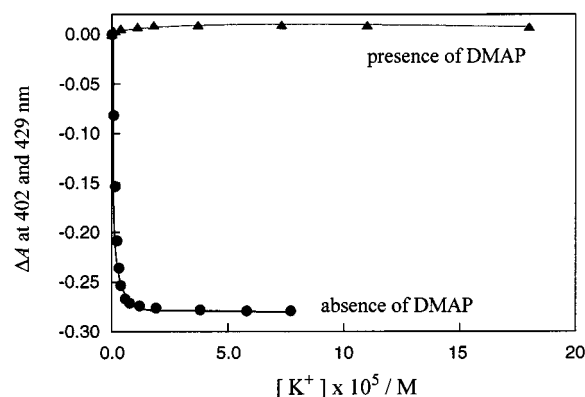


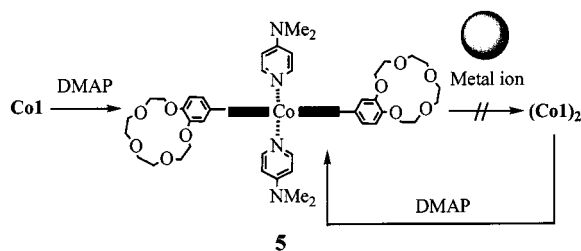
Figure 9. Plots of $[\text{K}^+]$ against ΔA for **Co1** in the absence and presence of DMAP in $\text{CHCl}_3/\text{MeCN}$, 2:1 at room temperature; $[\text{Co1}] = 1.9 \times 10^{-6} \text{ M}$, $[\text{DMAP}] = 0$ or $2.0 \times 10^{-2} \text{ M}$

Dimerization Control by Coordination at the Central Metal

In the case of six-coordinated metalloporphyrins such as **Co1**,^[19] the K^+ ion-induced dimerization may be competitive with coordination of the central metal atom. We thus examined the dimerization behavior of **Co1** in the presence of nitrogen-containing ligands. As seen with **Zn1**, addition of K^+ ions to **Co1** caused a blue shift of the Soret band from 402 to 389 nm, with an isosbestic point at 395 nm, as a result of *face-to-face* dimer-formation ($K = 3.3 \pm 0.9 \times 10^{18} \text{ M}^{-3}$). In the presence, on the other hand, of $2.0 \times 10^{-2} \text{ M}$ 4-dimethylaminopyridine (DMAP), the UV/vis spectrum of **Co1** showed no change upon addition of K^+ ions (Figure 9), indicating that *face-to-face* dimer-formation was completely inhibited by $2.0 \times 10^{-2} \text{ M}$ DMAP, probably due to the both-sides coordination of DMAP to Co^{II} porphyrin (Scheme 3). Interestingly, addition of DMAP to the *face-to-face* dimer of **Co1** in $\text{CHCl}_3/\text{CH}_3\text{CN}$ induced the monomerization of (**Co1**)₂ to **5**, through coordination of two DMAP molecules. This transformation can be followed by the spectral changes, including a Soret band red shift from 389 to 429 nm (Figure 10). The final absorption spectrum was identical with that of six-coordinated **Co1**.

Table 2. ^1H NMR spectroscopic data for **Zn1–3**

Compound	Chemical shifts (δ values)			
	<i>meso</i> -H	absence of K^+ β -H	<i>meso</i> -H	presence of K^+ β -H
Zn1	10.24	9.39, 9.12	10.27, 6.73	9.43, 8.89, 8.26, 7.38
Zn2	—	8.93, 8.87	—	8.92, 8.86
Zn3	10.13	9.33, 9.05, 8.95, 8.94	6.84	9.02, 8.74, 8.22, 7.44



Scheme 3. Complexation behavior of Co1

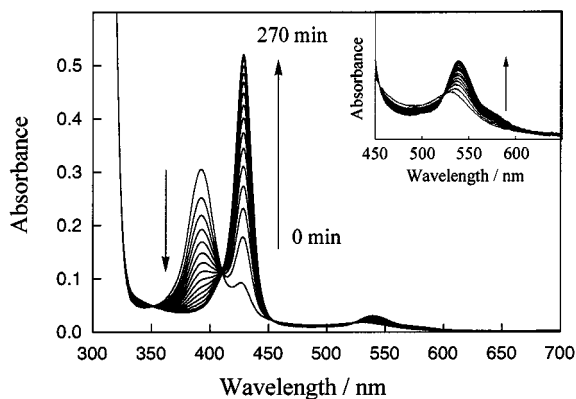


Figure 10. Change over time of absorption spectra of Co1 plus K^+ on complexation of DMAP in $CHCl_3/MeCN$, 2:1 at room temperature; $[Co1] = 1.9 \times 10^{-6}$ M, $[KClO_4] = 3.8 \times 10^{-5}$ M, $[DMAP] = 2.0 \times 10^{-2}$ M

Extended Molecular Assembly of Porphyrin

The UV/vis spectral changes of Zn4 upon addition of K^+ ions were more complicated (Figure 11). In the absence of metal ion, Zn4 exhibited split Soret bands due to exciton coupling, at 421 and 453 nm.^[10] On addition of K^+ ions up to 1.0×10^{-5} M, the intensities of the Soret band at 421 and 453 nm were decreased, and further addition resulted in a slight red shift of the Soret band to 423 from 421 nm, followed by an increase in its absorbance and a slight blue

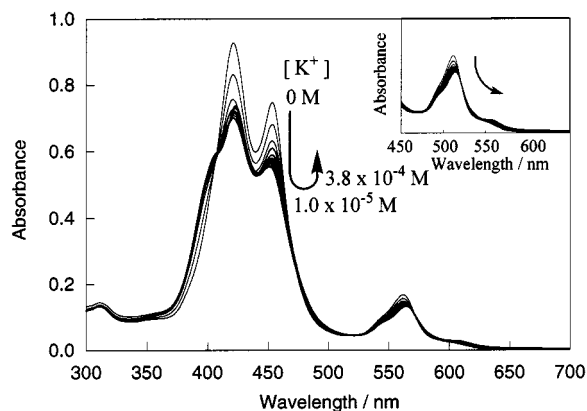


Figure 11. Absorption spectra of Zn4 on addition of $KClO_4$ in $CHCl_3/MeCN$, 2:1 at room temperature; $[Zn4] = 3.8 \times 10^{-6}$ M

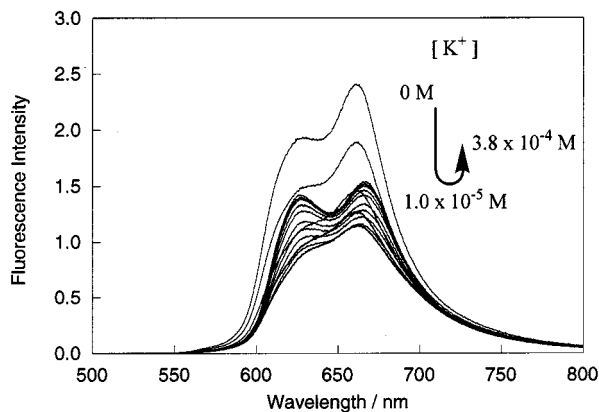


Figure 12. Fluorescence spectra of Zn4 on addition of $KClO_4$ in $CHCl_3/MeCN$, 2:1 at room temperature; $[Zn4] = 3.8 \times 10^{-6}$ M, $\lambda_{ex} = 408$ nm

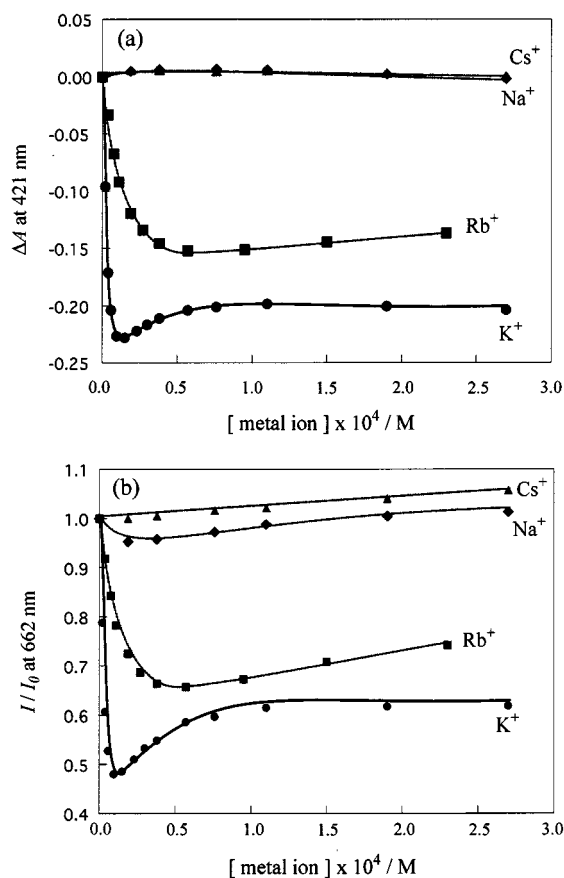


Figure 13. Plots of $[metal\ ion]$ against ΔA at 421 nm (a) and I/I_0 at 662 nm (b) for Zn4 in $CHCl_3/MeCN$, 2:1 at room temperature; $[Zn4] = 3.8 \times 10^{-6}$ M, $\lambda_{ex} = 408$ nm

shift of the Soret band to 451 from 453 nm, followed in turn by an decrease in its absorbance. In the course of these changes, a shoulder appeared at the high-energy side of the Soret band, with an isosbestic point at 408 nm. The fluorescence intensity changed in a complicated manner (Figure 12). On addition of K^+ ions up to 1.0×10^{-5} M, the fluorescence intensity at 628 (shoulder) and 662 nm was reduced, and further addition resulted in a slight shift of the

emission band to 626 from 628 nm (shoulder) and to 666 from 662 nm, followed by an increase in its fluorescence. The fluorescence quantum yields of **Zn1** and **Zn1** plus K^+ ions determined relative to ZnTPP (0.03)^[15] were 0.030, 0.009 ($[K^+] = 1.0 \times 10^{-5}$ M), and 0.012 ($[K^+] = 3.8 \times 10^{-4}$ M), respectively. Similar UV/vis and fluorescence spectral behavior was observed upon addition of Rb^+ ions, but not on addition of Cs^+ ions or Na^+ ions. Plots of $[K^+]$ against ΔA at 421 nm and I/I_0 at 662 nm for **Zn4** are shown in Figure 13, indicating a steep decrease in intensity upon addition of potassium ions up to 1.0×10^{-5} M, followed by a slight restoration upon further addition. These changes were in contrast to a rather monotonous and saturated fluorescence intensity decrease of **Zn1** on addition of potassium ions (Figure 5). In the UV/vis study, appearance of a shoulder on the high-energy side of the Soret band suggested the formation of *face-to-face* stacked diporphyrin, as for **Zn1**. It was therefore plausible that the intermolecular interaction mode of the appended crown ether with potassium ion might be the same for **Zn1** and **Zn4**, but the resultant molecular architectures for **Zn1** and for **Zn4** were entirely different. Whereas the complexation between two crown ether sites and K^+ ion resulted in *face-to-face* dimerization in the case of **Zn1**, such self-complementary complexation was impossible for **Zn4**, which thus tended to prefer linear extended aggregation. The observed complicated profiles of the UV/vis spectral and fluorescence intensity

changes for **Zn4** on addition of K^+ ions indicated multi-stage equilibria. The initial steep decrease in fluorescence intensity for complexation of **Zn4** with K^+ ion (Figure 13b) might suggest fluorescence quenching originating from the formation of the complexed *face-to-face* diporphyrin in **Zn4**. Subsequent slight increase in the fluorescence intensity might be caused by the interaction between the crown ethers at the edges of the linear aggregate and metal ions. A result in favor of this interpretation is to be found in Figure 5b, in which the fluorescence intensity was enhanced by interaction between Na^+ ions and crown ether sites in **Zn1**. Consistently with the proposed polymeric structure, the 1H NMR spectrum of **Zn4** (1.0 mM) became very broad on addition of potassium ions, and no assignment of signals was possible. The polymeric nature of the aggregate formed from **Zn4** was confirmed by a light-scattering measurement, which indicated a molecular weight of approximately 10^5 for the aggregate, corresponding to an aggregation number of ca. 50 (Scheme 4).

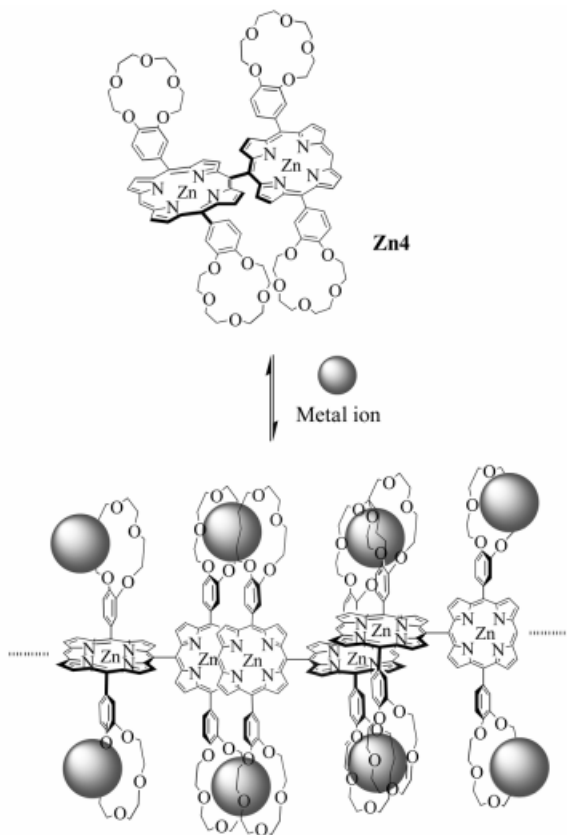
Conclusions

It has been demonstrated that strong *face-to-face* dimerization of 5,15-bis(benzo-15-crown-5) metalloporphyrins was effected through self-complementary interactions between K^+ ion and the two crown ethers and additional π - π interactions between the sterically uncongested metalloporphyrins. The dimer formation was found to be particularly sensitive to steric effects at the *meso*-position, which could be used for construction of a conformationally well defined dimer from **Zn3**. Moreover, dimer-to-monomer interconversion was achieved by addition of an excess of ligating base to (**Co1**)₂. Finally, a change in the aggregation mode, from dimerization to extended linear assembly, was observed for the *meso-meso* coupled diporphyrin **Zn4**.

Experimental Section

General: Starting chemicals were either prepared according to literature procedures or were commercially available and used without further purification. All solvents were purified and dried by standard methods. 1H NMR spectra (500 MHz) were recorded on a JEOL ALPHA-500 FT NMR spectrometer, chemical shifts being referenced to tetramethylsilane ($\delta = 0.00$). FAB mass spectra were measured on a JEOL HX-110 spectrometer by the positive-FAB ionization method with a 3-nitrobenzyl alcohol matrix. MALDI-TOF mass spectra were measured on a Shimadzu/KRATOS MALDI 4 spectrometer. UV/vis spectra were measured on a Shimadzu UV-2400PC UV/vis recording spectrophotometer. Fluorescence spectra were measured on a Shimadzu RF-5300PC spectrofluorophotometer. Aggregation behavior was studied with a light-scattering photometer (Otsuka Electronics ELS-800).

Porphyrin 1: 4'-Formyl-benzo-15-crown-5 (420 mg, 1.23 mmol) and 2,2'-dipyrrylmethane (180 mg, 1.23 mmol) were dissolved in $CHCl_3$ (80 mL). After addition of $BF_3 \cdot Et_2O$ (2.5 M in $CHCl_3$, 0.16 mL, 4.0 mmol) the solution was stirred for 2 h at room temperature under N_2 in the dark. DDQ (450 mg, 2.0 mmol) was then added to



Scheme 4. Possible structure of metal-assisted supramolecular assembly of **Zn4**

the solution, and stirring was continued for an additional 2 h. After addition of triethylamine, the reaction mixture was passed through an alumina column. Chromatography on a silica gel column (eluent 10% MeOH in CH₂Cl₂) gave porphyrin **1** (101 mg, 0.12 mmol, 20%): ¹H NMR (500 MHz, CDCl₃): δ = 10.29 (s, 2 H, *meso*-H), 9.38 (d, *J* = 5.0 Hz, 4 H, β-H), 9.12 (d, *J* = 5.0 Hz, 4 H, β-H), 7.89 (s, 2 H, Ar), 7.79 (d, *J* = 8.0 Hz, 2 H, Ar), 7.29 (d, *J* = 8.0 Hz, 2 H, Ar), 4.48–3.88 (m, 32 H, methylene), –3.10 (s, 2 H, inner NH). Mass (FAB): found 842.4, calcd. for C₄₈H₅₀N₄O₁₀, 842.9. UV/vis (CHCl₃/MeCN, 2:1): λ_{max} (log ε) = 410 (5.54), 504 (4.24), 540 (3.87), 577 (3.72), and 636 (3.25) nm. Fluorescence (CHCl₃/MeCN, 2:1): λ_{max} = 636 and 696 nm. C₄₈H₅₀N₄O₁₀: calcd. C 68.39, H 5.98, N 6.65; found C 68.27, H 5.95, N 6.68.

Zn1: The porphyrin **1** (40 mg, 0.047 mmol) was dissolved in CHCl₃ (20 mL). A saturated solution of Zn^{II} acetate in MeOH was added to the solution, and the resulting mixture was refluxed for 3 h and poured into water. The reaction mixture was washed several times with water and dried over anhydrous MgSO₄. Chromatography on a silica gel column (eluent 10% MeOH in CHCl₃) gave porphyrin **Zn1** (37 mg, 0.041 mmol, 87%): ¹H NMR (500 MHz, [D₆]DMSO): δ = 10.24 (s, 2 H, *meso*-H), 9.39 (d, *J* = 5.0 Hz, 4 H, β-H), 9.13 (d, *J* = 5.0 Hz, 4 H, β-H), 7.84 (s, 2 H, Ar), 7.82 (d, *J* = 8.0 Hz, 2 H, Ar), 7.30 (d, *J* = 8.0 Hz, 2 H, Ar), 4.49–3.87 (m, 32 H, methylene). Mass (FAB): found 906.5, calcd. for C₄₈H₄₈N₄O₁₀Zn, 906.3. UV/vis (CHCl₃/MeCN, 2:1): λ_{max} (log ε) = 415 (5.73), 545 (4.35), and 583 (3.68) nm. Fluorescence (CHCl₃/MeCN, 2:1): λ_{max} = 590 and 640 nm. C₄₈H₄₈N₄O₁₀Zn·0.1H₂O: calcd. C 63.25, H 5.37, N 6.15; found C 63.02, H 5.29, N 6.08.

Co1: This compound was prepared from **1** and Co^{II} acetate in 90% yield according to the procedure outlined above for **Zn1**: Mass (FAB): found 899.3, calcd. for C₄₈H₄₈N₄O₁₀Co, 899.9. UV/vis (CHCl₃:MeCN = 2:1): λ_{max} (log ε) = 402 (5.35), and 519 (4.18) nm. C₄₈H₄₈N₄O₁₀Co·0.5CH₂Cl₂: calcd. C 61.81, H 5.25, N 5.95; found C 61.58, H 5.24, N 6.22.

Ni1: This compound was prepared from **1** and Ni^{II} acetate in 94% yield according to the procedure outlined above for **Zn1**: ¹H NMR (500 MHz, CDCl₃): δ = 9.92 (s, 2 H, *meso*-H), 9.17 (d, *J* = 5.0 Hz, 4 H, β-H), 8.98 (d, *J* = 5.0 Hz, 4 H, β-H), 7.61 (s, 2 H, Ar), 7.59 (d, *J* = 8.0 Hz, 2 H, Ar), 7.20 (d, *J* = 8.0 Hz, 2 H, Ar), 4.44–3.85 (m, 32 H, methylene). Mass (FAB): found 899.6, calcd. for C₄₈H₄₈N₄O₁₀Ni, 899.6. UV/vis (CHCl₃/MeCN, 2:1): λ_{max} (log ε) = 404 (5.39), 516 (4.30), and 547 (3.93) nm. C₄₈H₄₈N₄O₁₀Ni·0.5H₂O: calcd. C 63.44, H 5.45, N 6.17; found C 63.49, H 5.31, N 6.19.

Pd1: This compound was prepared from **1** and Pd^{II} acetate in 71% yield according to the procedure outlined above for **Zn1**: ¹H NMR (500 MHz, CDCl₃): δ = 10.26 (s, 2 H, *meso*-H), 9.28 (d, *J* = 5.0 Hz, 4 H, β-H), 9.05 (d, *J* = 5.0 Hz, 4 H, β-H), 7.76 (s, 2 H, Ar), 7.74 (d, *J* = 8.0 Hz, 2 H, Ar), 7.27 (d, *J* = 8.0 Hz, 2 H, Ar), 4.48–3.87 (m, 32 H, methylene). Mass (FAB): found 947.3, calcd. for C₄₈H₄₈N₄O₁₀Pd, 947.4. UV/vis (CHCl₃/MeCN, 2:1): λ_{max} (log ε) = 407 (5.36), 514 (4.37), and 545 (3.84) nm. C₄₈H₄₈N₄O₁₀Pd·1.3CH₂Cl₂: calcd. C 55.97, H 4.83, N 5.37; found C 56.16, H 4.79, N 5.08.

Cu1: This compound was prepared from **1** and Cu^{II} acetate in 89% yield according to the procedure outlined above for **Zn1**: Mass (FAB): found 904.7, calcd. for C₄₈H₄₈N₄O₁₀Cu, 904.5. UV/vis (CHCl₃/MeCN, 2:1): λ_{max} (log ε) = 406 (5.56), 528 (4.28), and 561 (3.57) nm. C₄₈H₄₈N₄O₁₀Cu·0.5CH₂Cl₂: calcd. C 61.51, H 5.23, N 5.91; found C 61.58, H 5.15, N 5.72.

Porphyrin 2: 4'-Formyl-benzo-15-crown-5 (200 mg, 0.67 mmol) and 5-phenyldipyrrromethane (150 mg, 0.67 mmol) were dissolved in

CHCl₃ (50 mL). After addition of BF₃·Et₂O (2.5 M in CHCl₃, 0.1 mL, 2.5 mmol) the solution was stirred for 2 h at room temperature under N₂ in the dark. DDQ (230 mg, 1.0 mmol) was then added to the solution, and stirring was continued for an additional 2 h. After addition of triethylamine, the reaction mixture was passed through an alumina column. Chromatography on a silica gel column (eluent 10% MeOH in CHCl₃) gave porphyrin **2** (50 mg, 0.05 mmol, 15%): ¹H NMR (500 MHz, CDCl₃): δ = 8.89 (d, *J* = 5.0 Hz, 4 H, β-H), 8.83 (d, *J* = 5.0 Hz, 4 H, β-H), 8.21 (d, *J* = 8.0 Hz, 4 H, Ar), 7.79 (s, 2 H, Ar), 7.76 (d, *J* = 8.0 Hz, 2 H, Ar), 7.75 (d, *J* = 8.0 Hz, 2 H, Ar), 7.29 (d, *J* = 8.0 Hz, 2 H, Ar), 7.24 (d, *J* = 8.0 Hz, 4 H, Ar), 4.44–3.86 (m, 32 H, methylene), –2.77 (s, 2 H, inner NH). Mass (FAB): found 996.2, calcd. for C₆₀H₅₈N₄O₁₀, 995.1. UV/vis (CHCl₃/MeCN, 2:1): λ_{max} (log ε) = 417 (5.54), 510 (3.90), 540 (4.23), 572 (3.70), and 646 (3.48) nm. Fluorescence (CHCl₃/MeCN, 2:1): λ_{max} = 650 and 713 nm. C₆₀H₅₈N₄O₁₀: calcd. C 72.42, H 5.87, N 5.63; found C 72.46, H 5.92, N 5.76.

Zn2: This compound was prepared from **2** in 93% yield according to the procedure outlined above for **Zn1**: ¹H NMR (500 MHz, CDCl₃): δ = 8.94 (d, *J* = 5.0 Hz, 4 H, β-H), 8.88 (d, *J* = 5.0 Hz, 4 H, β-H), 8.22 (d, *J* = 8.0 Hz, 4 H, Ar), 7.81 (s, 2 H, Ar), 7.76 (d, *J* = 8.0 Hz, 2 H, Ar), 7.75 (d, *J* = 8.0 Hz, 2 H, Ar), 7.27 (d, *J* = 8.0 Hz, 2 H, Ar), 7.19 (d, *J* = 8.0 Hz, 4 H, Ar), 4.48–3.87 (m, 32 H, methylene). Mass (FAB): found 1060.1, calcd. for C₆₀H₅₆N₄O₁₀, 1058.5. UV/vis (CHCl₃/MeCN, 2:1): λ_{max} (log ε) = 425 (5.71), 557 (4.38), and 598 (4.11) nm. Fluorescence (CHCl₃/MeCN, 2:1): λ_{max} = 605 and 658 nm. C₆₀H₅₆N₄O₁₀Zn: calcd. C 68.08, H 5.33, N 5.29; found C 68.07, H 5.45, N 5.15.

Porphyrin 3: 4'-Formyl-benzo-15-crown-5 (1.0 g, 3.37 mmol), 2,2'-dipyrrylmethane (250 mg, 1.70 mmol), and 5-(4-hydroxyphenyl)dipyrrromethane (405 mg, 1.70 mmol) were dissolved in CHCl₃ (400 mL). After addition of BF₃·Et₂O (2.5 M in CHCl₃, 0.9 mL, 23 mmol), the solution was stirred for 2 h at room temperature under N₂ in the dark. DDQ (1.36 g, 6.0 mmol) was then added to the solution, and stirring was continued for an additional 8 h. After addition of triethylamine, the reaction mixture was passed through an alumina column. Chromatography on a silica gel column (eluent 10% MeOH in CH₂Cl₂) gave porphyrin **3** (100 mg, 0.11 mmol, 7%): ¹H NMR (500 MHz, CDCl₃): δ = 10.13 (s, 1 H, *meso*-H), 9.28 and 9.03 (d, *J* = 5.0 Hz, 4 H, β-H), 8.90 and 8.89 (d, *J* = 5.0 Hz, 4 H, β-H), 8.03 (d, *J* = 8.0 Hz, 2 H, Ar), 7.78–7.68 (m, 6 H, Ar and OH), 7.18 (d, *J* = 8.0 Hz, 2 H, Ar), 4.42–3.84 (m, 32 H, methylene), –3.01 (s, 2 H, inner NH). Mass (FAB): found 935.4, calcd. for C₅₄H₅₄N₄O₁₁, 935.0. UV/vis (CHCl₃/MeCN, 2:1): λ_{max} (log ε) = 413 (5.53), 505 (3.90), 534 (4.23), 563 (3.70), and 637 (3.48) nm. Fluorescence (CHCl₃/MeCN, 2:1): λ_{max} = 647 and 707 nm. C₅₄H₅₄N₄O₁₁·0.9CH₂Cl₂: calcd. C 65.21, H 5.56, N 5.53; found C 65.45, H 5.87, N 5.23.

Zn3: This compound was prepared from **3** in 95% yield according to the procedure outlined above for **Zn1**: ¹H NMR (500 MHz, CDCl₃): δ = 10.3 (s, 1 H, *meso*-H), 10.21 (s, 1 H, *meso*-H), 9.37 (d, *J* = 4.5 Hz, 2 H, β-H), 9.13 (d, *J* = 4.5 Hz, 2 H, β-H), 9.03 (d, *J* = 4.5 Hz, 2 H, β-H), 9.02 (d, *J* = 4.5 Hz, 2 H, β-H), 8.07 (d, *J* = 8.0 Hz, 4 H, Ar), 7.82 (s, 2 H, Ar), 7.76 (d, *J* = 8.0 Hz, 2 H, Ar), 7.27 (d, *J* = 8.0 Hz, 2 H, Ar), 7.22 (d, *J* = 8.0 Hz, 4 H, Ar), 4.48–3.87 (m, 32 H, methylene). Mass (FAB): found 999.5, calcd. for C₅₄H₅₂N₄O₁₁Zn, 998.4. UV/vis (CHCl₃/MeCN, 2:1): λ_{max} (log ε) = 422 (5.71), 551 (4.38), and 590 (4.00) nm. Fluorescence (CHCl₃/MeCN, 2:1): λ_{max} = 600 and 650 nm. C₅₄H₅₂N₄O₁₁Zn·0.2CH₂Cl₂: calcd. C 60.30, H 4.98, N 5.10; found C 60.31, H 5.24, N 4.82.

Diporphyrin Zn4: Porphyrin **Zn1** (50 mg, 0.06 mmol) was dissolved in 5% MeOH in CHCl₃ (100 mL). After addition of AgPF₆ (0.1 M in MeCN, 3.0 mL, 0.30 mmol), the solution was stirred for 8 h at room temperature in the dark. The reaction mixture was washed several times with water and dried over anhydrous MgSO₄. Chromatography on a silica gel column (eluent 10% MeOH in CH₂Cl₂) gave porphyrin **Zn4** (13 mg, 0.007 mmol, 13%): ¹H NMR (500 MHz, [D₆]DMSO): δ = 10.37 (s, 2 H, *meso*-H), 9.52 (d, *J* = 5.0 Hz, 4 H, β-H), 9.02 (d, *J* = 5.0 Hz, 4 H, β-H), 8.62 (d, *J* = 5.0 Hz, 4 H, β-H), 7.89 (d, *J* = 5.0 Hz, 4 H, β-H), 7.80–7.67 (m, 8 H, Ar), 7.26 (d, *J* = 8.0 Hz, 4 H, Ar), 4.38–3.44 (m, 64 H, methylene). Mass (MALDI-TOF): found 1809.1, calcd. for C₉₆H₉₄N₈O₂₀Zn₂, 1810.6. UV/vis (CHCl₃/MeCN, 2:1): λ_{max} (log ε) = 421 (5.39), 453 (5.60), and 562 (4.65) nm. Fluorescence (CHCl₃/MeCN, 2:1): λ_{max} = 628 and 662 nm. C₉₆H₉₄N₈O₂₀Zn₂·6.5H₂O: calcd. C 59.80, H 5.61, N 5.81; found C 60.05, H 5.39, 5.52.

- [1] J.-M. Lehn, *Angew. Chem. Int. Ed. Engl.* **1988**, *27*, 89–112; G. M. Whitesides, J. P. Mathias, C. T. Seto, *Science* **1991**, *254*, 1312–1319; D. Philp, J. F. Stoddart, *Angew. Chem. Int. Ed. Engl.* **1996**, *35*, 1154–1196; M. Fujita, *Chem. Soc. Rev.* **1998**, *27*, 417–425.
- [2] L. D. Sarson, K. Ueda, M. Takeuchi, S. Shinkai, *Chem. Commun.* **1996**, 619–620; K. Kobayashi, M. Koyanagi, K. Endo, H. Masuda, Y. Aoyama, *Chem. Eur. J.* **1998**, *4*, 417–424; U. Michelsen, C. A. Hunter, *Angew. Chem. Int. Ed.* **2000**, *39*, 764–767.
- [3] K. Maruyama, A. Osuka, *Pure Appl. Chem.* **1990**, *62*, 1511–1520; M. R. Wasielewski, *Chem. Rev.* **1992**, *92*, 435–461; A. Osuka, N. Mataga, T. Okada, *Pure Appl. Chem.* **1997**, *69*, 797–802.
- [4] M. D. Ward, *Chem. Soc. Rev.* **1997**, *26*, 365–375; T. Hayashi, H. Ogoshi, *Chem. Soc. Rev.* **1997**, *26*, 355–364.
- [5] I. Tabushi, *Coord. Chem. Rev.* **1988**, *86*, 1–42; L. G. Mackay, R. S. Wyllie, J. K. M. Sanders, *J. Am. Chem. Soc.* **1994**, *116*, 3141–3142; J. P. Collman, P. S. Wagenknecht, J. E. Hutchison, *Angew. Chem. Int. Ed. Engl.* **1994**, *33*, 1537–1554.
- [6] M. J. Gunter, D. C. R. Hockless, M. R. Johnston, B. W. Skelton, A. H. White, *J. Am. Chem. Soc.* **1994**, *116*, 4810–4823; H. Harriman, J.-P. Sauvage, *Chem. Soc. Rev.* **1996**, *25*, 41–48; J. Fun, J. A. Whiteford, B. Oleynyuk, M. D. Levin, P. J. Stang, E. B. Fleischer, *J. Am. Chem. Soc.* **1999**, *121*, 2741–2752; N. Solladio, J.-C. Chambron, J.-P. Sauvage, *J. Am. Chem. Soc.* **1999**, *121*, 3684–3692.
- [7] C. A. Hunter, L. D. Sarson, *Angew. Chem. Int. Ed. Engl.* **1994**, *33*, 2313–2316; X. Chi, J. G. Guerin, R. A. Haycock, C. A. Hunter, L. D. Sarson, *J. Chem. Soc., Chem. Commun.* **1995**, 2567–2569; C. A. Hunter, R. K. Hyde, *Angew. Chem. Int. Ed. Engl.* **1996**, *35*, 1936–1936; M. Gardner, A. J. Guerin, C. A. Hunter, U. Michelsen, C. Rotger, *New J. Chem.* **1999**, 309–316; R. A. Haycock, C. A. Hunter, D. A. James, U. Michelsen, L. R. Sutton, *Org. Lett.* **2000**, *2*, 2435–2438; R. A. Haycock, A. Yartsev, U. Michelsen, V. Sundström, C. A. Hunter, *Angew. Chem. Int. Ed.* **2000**, *39*, 3616–3619; P. N. Taylor, H. L. Anderson, *J. Am. Chem. Soc.* **1999**, *121*, 11538–11545; Y. Kobuke, H. Miyaji, *J. Am. Chem. Soc.* **1994**, *116*, 4111–4112; Y. Kobuke, H. Miyaji, *Bull. Chem. Soc. Jpn.* **1996**, *69*, 3563–3569; K. Ogawa, Y. Kobuke, *Angew. Chem. Int. Ed.* **2000**, *39*, 4070–4073; A. Ambroise, J. Li, L. Yu, J. S. Lindsey, *Org. Lett.* **2000**, *17*, 2563–2566; J. N. H. Reek, A. P. H. J. Schenning, A. W. Bosman, E. W. Meijer, M. J. Crossley, *Chem. Commun.* **1998**, 11–12; T. Imamura, K. Fukushima, *Coord. Chem. Rev.* **2000**, *198*, 133–156; J. Wojaczynski, L. Latos-Grazynski, *Coord. Chem. Rev.* **2000**, *204*, 113–171.
- [8] M. Hisatome, K. Ikeda, S. Kishibata, K. Yamakawa, *Chem. Lett.* **1993**, 1357–1360; C. M. Drain, R. Fischer, E. G. Nolen, J.-M. Lehn, *J. Chem. Soc., Chem. Commun.* **1993**, 243–245; Ikeda, C.; Nagahara, N.; Motegi, E.; N. Yoshioka, Inoue, H. *Chem. Commun.* **1999**, 1759–1760; Y. Diskin-Posner, I. Goldberg, *Chem. Commun.* **1999**, 1961–1962; N. Nagata, S. Kugimiya, Y. Kobuke, *Chem. Commun.* **2000**, 1389–1390; T. S. Balaban, A. Eichhöfer, J.-M. Lehn, *Eur. J. Org. Chem.* **2000**, 4047–4057; M. C. Calama, P. Timmerman, D. N. Reinhoudt, *Angew. Chem. Int. Ed.* **2000**, *39*, 755–758.
- [9] V. Thanabal, V. Krishnan, *J. Am. Chem. Soc.* **1982**, *104*, 3643–3650; V. Thanabal, V. Krishnan, *Inorg. Chem.* **1982**, *21*, 3606–3613; B. Maiya, V. Krishnan, *Inorg. Chem.* **1985**, *24*, 3253–3257; T. K. Chandrashekar, H. van Willigen, M. H. Ebersole, *J. Phys. Chem.* **1985**, *89*, 3453–3459.
- [10] A. Osuka, H. Shimidzu, *Angew. Chem. Int. Ed. Engl.* **1997**, *36*, 135–137; A. Nakano, A. Osuka, I. Yamazaki, T. Yamazaki, Y. Nishimura, *Angew. Chem. Int. Ed.* **1998**, *37*, 3023–3027; N. Yoshida, H. Shimidzu, A. Osuka, *Chem. Lett.* **1998**, 55–56; N. Aratani, A. Osuka, Y. H. Kim, D. H. Jeong, D. Kim, *Angew. Chem. Int. Ed.* **2000**, *39*, 1458–1462; N. Yoshida, N. Aratani, A. Osuka, *Chem. Commun.* **2000**, 197–198; A. Nakano, T. Yamazaki, Y. Nishimura, I. Yamazaki, A. Osuka, *Chem. Eur. J.* **2000**, *6*, 3251–3271; A. Tsuda, A. Nakano, H. Furuta, H. Yamochi, A. Osuka, *Angew. Chem. Int. Ed.* **2000**, *39*, 558–561; A. Tsuda, H. Furuta, A. Osuka, *Angew. Chem. Int. Ed.* **2000**, *39*, 2549–2552.
- [11] R. E. Fenna, B. W. Matthews, *Nature* **1975**, *258*, 573–577; J. Deisenhofer, O. Epp, K. Miki, R. Huber, H. Michel, *J. Mol. Biol.* **1984**, *180*, 385–398; O. Epp, K. Miki, R. Huber, H. Michel, *Nature* **1985**, *318*, 618–624; N. Krauss, W. Hinrichs, I. Witt, P. Fromme, W. Pritzkow, Z. Dauter, C. Betzel, K. S. Wilson, H. T. Witt, W. Saenger, *Nature* **1993**, *361*, 326–331; G. McDermott, S. M. Prince, A. A. Freer, A. M. Hawthornthwaite-Lawless, M. Z. Papiz, R. J. Cogdell, N. W. Isaacs, *Nature* **1995**, *374*, 517–521; P. Jordan, P. Fromme, H.-T. Witt, O. Klukas, W. Saenger, N. Kraus, *Nature* **2001**, *411*, 909–917.
- [12] D. E. Williams, S. E. Hale, R. T. Okita, B. S. S. Masters, *J. Biol. Chem.* **1984**, *259*, 14600–14608; F. P. Guengerich, T. L. Macdonald, *Acc. Chem. Res.* **1984**, *17*, 9–16; D. Xia, C.-A. Yu, H. Kim, J. Z. Xia, A. M. Kachurin, L. Zhang, L. Yu, J. Deisenhofer, *Science* **1997**, *277*, 60–66.
- [13] J.-H. Fuhrhop, K. M. Smith, In *Porphyrins and Metalloporphyrins*; (Ed.: M. Smith); Elsevier, Amsterdam, **1975**, p757–p869.
- [14] Preliminary communication: H. Shinmori, A. Osuka, *Tetrahedron Lett.* **2000**, *41*, 8527–8531.
- [15] P. G. Seybold, M. Goutermann, *J. Mol. Spectrosc.* **1969**, *31*, 1–13.
- [16] A. Job, *Ann. Chim.* **1928**, *9*, 113–203.
- [17] H. K. Frensdorff, *J. Am. Chem. Soc.* **1971**, *93*, 600–606; J. J. Christensen, D. J. Eatough, R. M. Izatt, *Chem. Rev.* **1974**, *74*, 351–384.
- [18] C. A. Hunter, J. K. M. Sanders, *J. Am. Chem. Soc.* **1990**, *112*, 5525–5534.
- [19] J. S. Summers, A. M. Stolzenberg, *J. Am. Chem. Soc.* **1993**, *115*, 10559–10567.

Received September 24, 2001
[O01455]